Axial Compressive Strength of Carbon Fiber

TADASHI OHSAWA, MINORU MIWA,* and MASATO KAWADE,
Faculty of Engineering, Gifu University, Yanagido, Gifu 501-11, Japan, and EIKI TSUSHIMA, *Corporate Research and Development Laboratory, Toa Nenryo Kogyo Co., Ltd., Nishi-tsurugaoka 1-chome, Ohi-machi, Iruma-gun, Saitama 354, Japan*

Synopsis

Efforts were made to estimate the axial compressive strengths of carbon fibers from the fiber fragment lengths produced by subjecting to a strain greater than the fiber ultimate strain for PAN-based and pitch-based carbon fibers. The estimated compressive strength of carbon fibers decreases with increasing temperature in a temperature range from room temperature to 100°C. This decrease in compressive strength may be accounted for by a decrease in the radial compressing force. The real compressive strength, determined by extrapolating a linear relationship between the estimated compressive strength and the radial compressing force, is approximately 25–60% of tensile strength for PAN-based fibers, while it is approximately 10–35% for pitch-based fibers.

INTRODUCTION

Relationship between the mechanical properties (strength, fracture strain, and modulus) of composites in tension and those of the fibers used as reinforcement have been studied both experimentally and theoretically in fairly great detail. However, in spite of the fact that the compressive characteristics of composites depend on the characteristics of reinforcing fibers, there is almost no study on the mechanical properties of composites in compression because it is difficult to determine accurately the axial compressive properties of reinforcing fibers.

Efforts were made to determine the axial compressive properties of reinforcing fibers. Sinclair and Chamis[1] estimated the compressive modulus and strength of carbon fibers from those of unidirectional composites according to a rule of mixtures. Jones and Johnson[2] estimated the compressive fracture strain of carbon fibers from the radius of curvature of the fiber loop at the point of maximum strain using the elastica method. Moreover, Hawthorne and Teghtsoonian[3] studied the axial compression fracture of carbon fibers by embedding a single fiber in the epoxy resin and compressing the specimens parallel to the fiber axis. They identified the earliest stages of fracture by careful optical monitoring of the fiber surface and estimated the fiber axial compression failure strengths from both the earliest fracture strain and the tensile modulus.

*To whom correspondence should be addressed.

Journal of Applied Polymer Science, Vol. 39, 1733–1743 (1990)
 CCC 0021-8995/90/081733-11$04.00

There are some questions in the above-mentioned studies. In the report by Sinclair and Chamis[1] a rule of mixtures doesn't always hold in compression. In the fiber loop,[2] the fiber doesn't always fail in the compression side of fiber. Hawthorne and Teghtsoonian[3] used the tensile modulus to estimate the fiber axial compression failure strengths. However, it is doubtful that compressive modulus is equal to the tensile modulus and the linearity holds in the compressive stress–strain curves.

In this paper, efforts were made to determine accurately the fiber axial compressive strengths using the yield shear strength at the fiber–matrix interphase. Namely, if a sufficiently long fiber is embedded in the resin matrix and the system is compressed, the fiber eventually breaks into many pieces, on the assumption that a theory according to Kelly and Tyson,[4,5] while assuming that the yield shear strength at the fiber-matrix interphase is constant, may be applied to the system in compression. By measuring the lengths of the broken pieces, we estimated the fiber axial compressive strengths.

MEASUREMENTS

Principle

If a sufficiently long fiber is embedded in the resin matrix and the system is subjected to a tensile strain greater than the fiber ultimate strain, the fiber eventually breaks into many pieces. Assuming that the fiber strength is uniform along the length of the fiber, the critical fiber length $(l_c)_{\text{ten}}$ in tension is given as follows[6]:

$$(l_c)_{\text{ten}} = \tfrac{4}{3}(\bar{l})_{\text{ten}} \tag{1}$$

where $(\bar{l})_{\text{ten}}$ is the mean fragment length.

Moreover, according to Kelly and Tyson[4,5] the relationship between critical fiber length $(l_c)_{\text{ten}}$ and the tensile strength of fiber $(\sigma_f)_{\text{ten}}$ results in the following equation:

$$(l_c)_{\text{ten}} = \frac{(\sigma_f)_{\text{ten}} \cdot d}{2\tau} \tag{2}$$

where τ is the yield shear strength at the fiber–matrix interphase and d is the diameter of the fiber. Accordingly, τ can be determined from eqs. (1) and (2) by measuring mean fragment length $(\bar{l})_{\text{ten}}$ in tension.

When the above-mentioned specimen is compressed in the direction of the fiber axis, we assumed that the yield shear strength of the same value as that in tension, but the working direction is the reverse. Therefore, if the specimen is compressed, the fiber eventually breaks into many pieces in the same manner as in the case of tension. Measuring the mean fragment in compression $(\bar{l})_{\text{comp}}$, the critical fiber length in compression $(l_c)_{\text{comp}}$ is given as follows:

$$(l_c)_{\text{comp}} = \tfrac{4}{3}(\bar{l})_{\text{comp}} \tag{3}$$

Moreover, according to the above-mentioned assumption, the following equation holds:

$$(l_c)_{\text{comp}} = \frac{(\sigma_f)_{\text{comp}} \cdot d}{2\tau} \tag{4}$$

where $(\sigma_f)_{\text{comp}}$ is the fiber axial compressive strength. As τ and d in eq. (4) are the same values as those in eq. (2), the fiber axial compressive strength $(\sigma_f)_{\text{comp}}$ can finally be estimated from the following equation:

$$\frac{(\sigma_c)_{\text{comp}}}{(\sigma_c)_{\text{ten}}} = \frac{(l_c)_{\text{comp}}}{(l_c)_{\text{ten}}} \tag{5}$$

$(l_c)_{\text{ten}}$ and $(l_c)_{\text{comp}}$ in eq. (5) are characteristic values for a given composite system under the same environmental condition. Therefore, when critical fiber lengths will be determined under the same environmental condition, eq. (5) shows that the ratio of fiber compressive strength to tensile strength is given by the ratio of critical fiber length in compression to that in tension.

It is impossible to obtain the length dependence of compressive strength of carbon fiber for the present. Accordingly, to rough approximation, assuming that the ratio compressive strength to tensile strength is the same value regardless of the fiber length, it is conceivable that the compressive strength $(\sigma_f)_{\text{comp}}$ obtained by substituting the tensile strength at a given length into eq. (5) is the estimated compressive strength corresponding to the tensile strength.

In this experiment, to accurately give the fiber the tensile strain, a rectangular (beam) in which a long fiber was embedded at a constant tension in the neighborhood of the surface prepared [Fig. 1 (a)] and the four-point bending method was adopted. If the side having a fiber of the specimen is bent outside, the fiber is elongated. As the fiber is evenly strained within the distance between the loading heads C and D [Fig. 1 (b)], the fragment lengths of the fiber can be measured over the section C–D.

Second, if the side having a fiber of the specimen is bent inside, the fiber is compressed. However, when the compressive fracture strain of carbon fibers

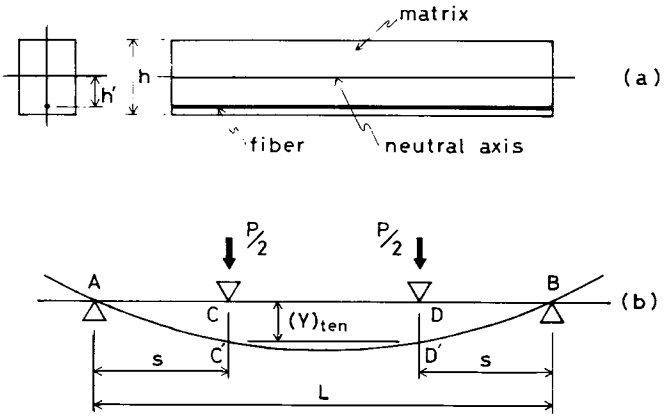

Fig. 1. Schematic diagram of four-point bending test in tension.

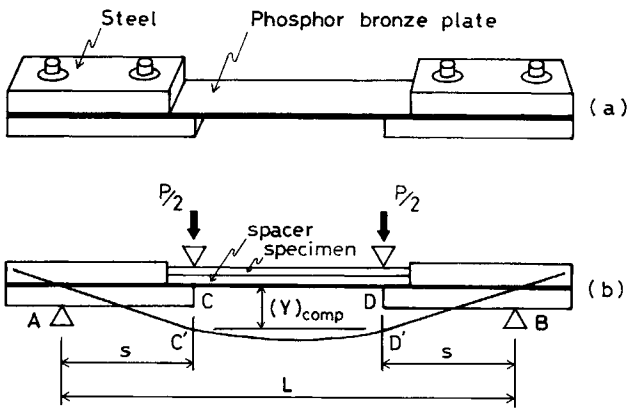

Fig. 2. Schematic diagram of four-point bending test in compression.

is larger than the tensile ultimate strain, the fracture of rectangular beam is often preceded by the tensile fracture of the resin matrix and the experiments becomes a failure in spite of all the effort. Therefore, an equipment was devised to compress the specimen [Fig. 2 (a)]. The specimen embedding a long fiber was set on the phosphor bronze plate between the loading heads C and D of the equipment. Accordingly, a laminated beam consisting of both the phosphor bronze plate and the specimen was composed. The thickness of phosphor bronze plate is 1 mm. Young's modulus of phosphor bronze plate is nearly two figures greater than that of the resin matrix. When the laminated beam is bent, it always has the neutral plane in the neighborhood of the upper surface of phosphor bronze plate. Consequently, the specimen is compressed only.

Using the method shown in Figure 1(b), the drop $(Y)_{ten}$ of heads C and D required to a constant tensile strain $(\epsilon_f)_{ten}$ is given by the following equation according to the bending theory:

$$(Y)_{ten} = \frac{(\epsilon_f)_{ten}}{6h'} \cdot s \cdot (3L - 4s) \tag{6}$$

where h' is the distance between the fiber and the neutral axis, L is the span length, and S is the distance between the lower supporting point A (or B) and the upper loading head C (or D). Similarly, using the method shown in Figure 2(b), the drop $(Y)_{comp}$ required to give a constant compressive strain $(\epsilon_f)_{comp}$ is given by

$$(Y)_{comp} = \frac{(\epsilon_f)_{comp}}{2h'} \cdot s \cdot (L - 2s) \tag{7}$$

In compressive experiments, thinner specimens were preferred to be profitable the observations of fiber fragments under the optical microscope. In order to secure the required value of h', a spacer made of the same material as the resin matrix was inserted between the specimen and the phosphor bronze plate.

TABLE I
Mechanical Properties of Materials (at 20°C).[a]

Materials	Tensile strength (GPa)	Young's modulus (GPa)	Breaking strain (%)	Diameter (μm)
Carbon fiber				
Pitch-based				
Carbonized fiber HTX	3.34	230	1.46	10.1
Graphitized fiber HMX	4.33	482	0.90	10.1
PAN-based				
Carbonized fiber T-300	3.50	206	1.70	7.1
Graphitized fiber M-40	2.88	388	0.80	7.1
Matrix				
Epoxy resin	0.068	1.9	8.8	—

[a]Gauge length for fiber, 5 mm; HTX and HMX are Tonen's pitch based high performance carbon fibers. They are the materials under developing.

Preparation of Specimen

The fibers used in this study were PAN-based carbon fibers (Toray, Torayca 7.1 μm in diameter) and pitch-based carbon fibers (Toa Nenryo Kogyo, Tonen 10.1 μm in diameter). Moreover, carbonized (higher strength type) and graphitized fibers (higher modulus type) were respectively used (Table I). Matrix material was an epoxy resin (Epikote 828, Yuka Shell). Epoxy resin, 100 parts, was mixed with 10 parts of an amine hardening agent (S-Cure 661, Nihon Kayaku). The mixture was agitated thoroughly and then defoamed under vaccum for about 30 min. This mixture was poured into a mold holding a fiber at a constant tension and subjected to curing at 65°C for 17 h and postcuring at 140°C for 5 h. The specimen was then allowed to cool to room temperature at a cooling rate of about 0.5°C/min. The dimension of the mold resulted in a specimen which measured 13 mm in thickness, 10 mm in width, and 210 mm in length for the tensile experiments, and 4, 10, and 100 mm for the compression, respectively.

The specimens prepared in this manner were submitted to measurement of fragment length; each specimen was subjected to a tensile (or compressive) strain of 4% at a drop rate of the upper heads of 10 mm/min. Span length L was 180 mm. The distance S between points A (or B) and C (or D) is 50 mm. In order to investigate the effect of radially compressing force on the fiber axial compressive strength, measurements were made at intervals of 20°C from 20 to 140°C. Over 1000 fragments were examined for each experimental condition.

RESULTS AND DISCUSSION

The photographs of fiber fragments of the specimen compressed by the above-mentioned method are shown in Figure 3. The fiber is broken into a number of fragments. In the fiber breaking at 20°C [Fig. 3 (a)], the fiber fractures without the buckling. At 140°C [Fig. 3 (b)], the fiber buckles near the fracture point and the fracture appearances are remarkably different from those at 20°C. Namely, it is conceivable that the fiber is buckled by the

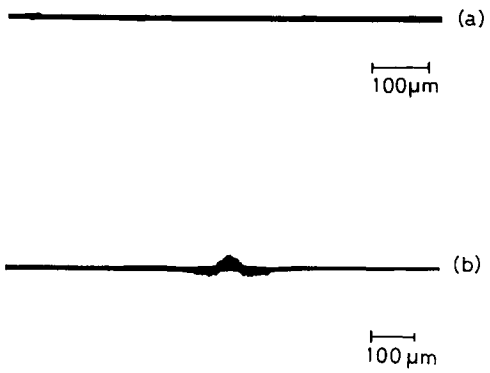

Fig. 3. Photographs of fiber breaking points in compression test (pitch-based carbonized fiber, HTX): (a) at 20°C; (b) at 140°C.

decrease in the radial force compressing the fiber owing to both the decrease in residual thermal stress and Young's modulus of the resin matrix. Figure 4 illustrates typical distribution of fiber fragment length. Similar results were obtained at various temperatures. The relationship between the critical fiber length $(l_c)_{ten}$ in tension obtained from the mean fragment length $(\bar{l})_{ten}$ according to eq. (1) and the temperature is shown in Figure 5. Moreover, the relationship between the critical fiber length $(l_c)_{comp}$ in compression obtained from the mean fragment length $(\bar{l})_{comp}$ in compression according to eq. (3) and the temperature is shown in Figure 6. Figure 7 shows the relationship between the value of fiber axial compressive strength estimated from the critical fiber length $(l_c)_{ten}$ (Fig. 5) in tension and the critical fiber length $(l_c)_{comp}$ (Fig. 6) in compression according to eq. (5) and the temperature. With these systems, the estimated compressive strength decreases with increasing temperature at a temperature range lower than 100°C. As the real axial compressive strength of carbonized and graphited fiber ought not to depend on the temperature at a

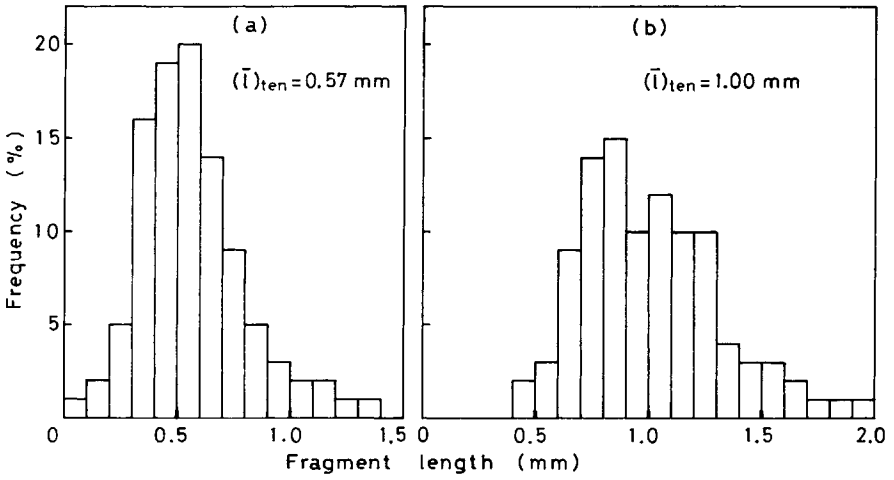

Fig. 4. Distribution of fragment length (pitch-based carbonized fiber, HTX): (a) at 40°C; (b) at 100°C.

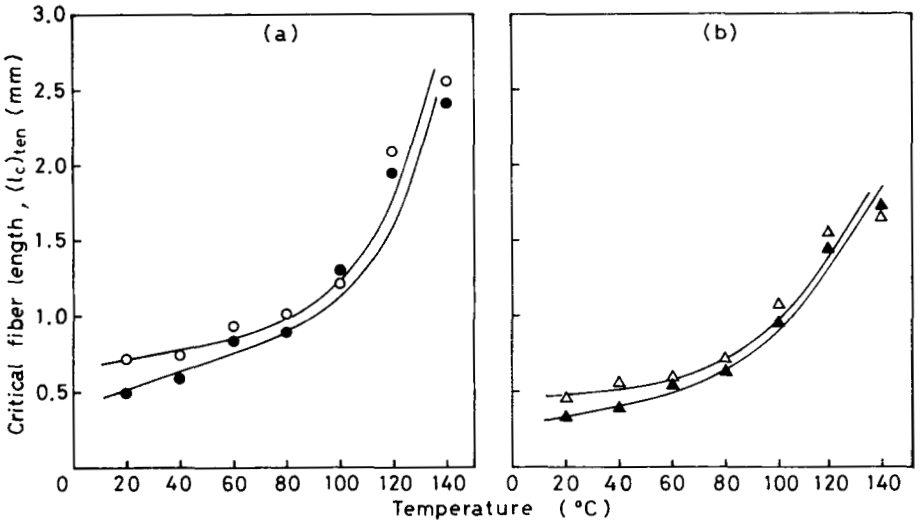

Fig. 5. Relation between temperature and critical fiber length in tension: (a) pitch-based carbon fiber; (b) PAN-based carbon fiber; (○) carbonized fiber, HTX; (●) graphitized fiber, HMX; (△) carbonized fiber, T-300; (▲) graphitized fiber, M-40.

temperature ranges of 20–100°C, it is conceivable that the radial force compressing the fiber decreased by both the decreases in residual thermal stress and Young's modulus of the resin matrix with increasing temperature may cause a temperature dependence of the estimated value of the fiber axial compressive strength. The thermal stress was produced by the difference in thermal expansion coefficient between fiber and resin. The estimated compressive strength increases greatly with increasing temperature above 120°C. It is

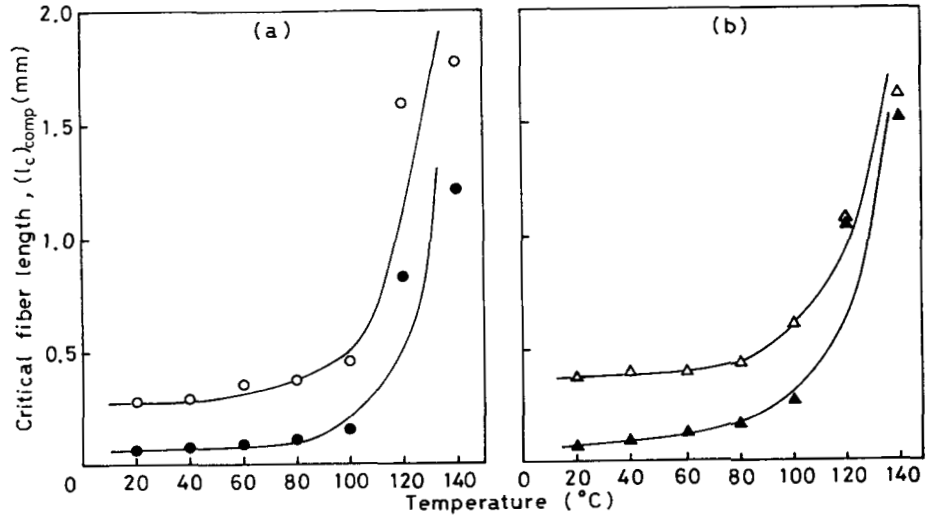

Fig. 6. Relation between temperature and critical fiber length in compression: (a) pitch-based carbon fiber; (b) PAN-based carbon fiber; (○) carbonized fiber, HTX; (●) graphitized fiber, HMX; (△) carbonized fiber, T-300; (▲) graphitized fiber, M-40.

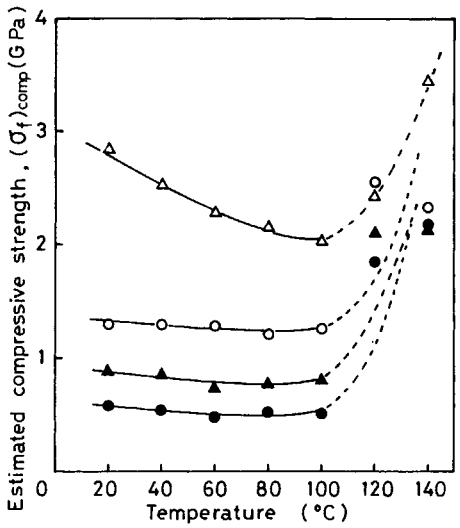

Fig. 7. Relation between temperature and estimated compressive strength: (○) pitch-based carbonized fiber, HTX; (●) pitch-based graphitized fiber, HMX; (△) PAN-based carbonized fiber, T-300; (▲) PAN-based graphitized fiber, M-40.

conceivable that this result may be caused by not satisfying the conditions for application of the above-mentioned eq. (5). As shown in Figure 3, when the specimen is compressed, the fiber buckles owing to the greater decrease in the Young's modulus of resin matrix. Accordingly, further details are discussed for the results obtained at temperature range lower than 100°C.

When a fiber is embedded in the resin and the system is allowed to cure, the thermal stress $(P)_T$ working perpendicularly on the fiber–resin interface is approximately given by the following equation[6,7]:

$$(P)_T \fallingdotseq \frac{\alpha_m \cdot E_m \cdot \Delta T}{1 + \nu_m} \tag{8}$$

where α is the thermal expansion coefficient, E is the Young's modulus, ν is the Poisson's ratio, ΔT is the difference in temperature from molding temperature, and the subscript m denotes matrix. Figure 8 shows the relationship between the thermal stress $(P)_T$ obtained by eq. (8). The thermal expansion coefficient (α_m), Young's modulus (E_m), and Poisson's ratio (ν_m) required to calculate the thermal stress $(P)_T$ are shown in Table II. Figure 9 shows the relationship between the estimated compressive strength and the thermal stress. It is obtained from the estimated compressive strength of the fiber–temperature relationship (Fig. 7) and the thermal stress–temperature relationship (Fig. 8). The estimated compressive strength of carbonized and graphitized fibers decreases linearly with decreasing thermal stress.

It is conceivable that the real compressive strength of carbonized and graphitized fiber is the strength when the radial compressing force; i.e., the residual thermal stress in this experiment is zero. Accordingly, we considered the value obtained by extrapolating the straight line in Figure 9 to $(P)_T = 0$ as the real compressive strength of carbonized and graphitized fiber and

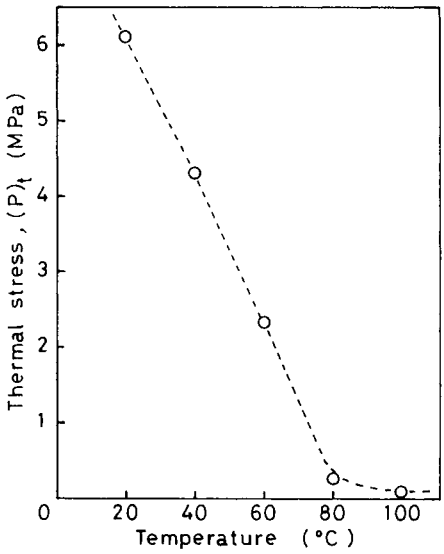

Fig. 8. Relation between temperature and thermal stress.

TABLE II
Properties of Epoxy Resin at Various Temperatures

Temperature (°C)	20	40	60	80	100	120	140
Thermal expansion coefficient α_m ($\times 10^{-5}$/°C)	6.1	7.2	8.1	14.3	14.7	15.2	15.2
Young's modulus E_m (GPa)	1.90	1.80	1.74	0.11	0.02	0.01	0.01
Poisson's ratio ν_m	0.30	0.33	0.35	0.38	0.40	0.43	0.45

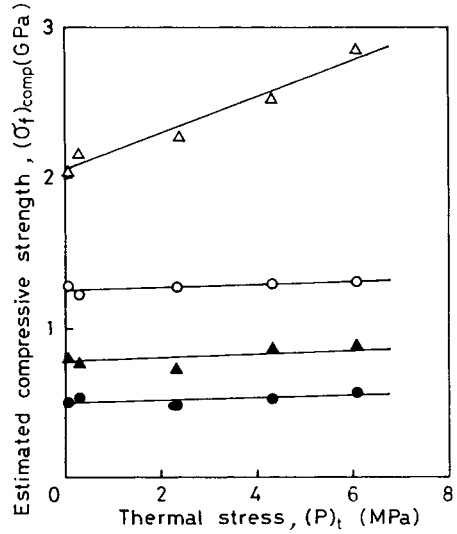

Fig. 9. Relation between thermal stress and estimated compressive strength: (○) pitch-based carbonized fiber, HTX; (●) pitch-based graphitized fiber, HMX; (△) PAN-based carbonized fiber, T-300; (▲) PAN-based graphitized fiber, M-40.

TABLE III
Tensile and Estimated Compressive Strength of Carbon Fiber

Carbon fiber	Pitch-based		PAN-based	
	Carbonized fiber HTX	Graphitized fiber HMX	Carbonized fiber T-300	Graphitized fiber M-40
Tensile strength $(\sigma_f)_{ten}$ (GPa)	3.34	4.33	3.50	2.88
Estimated compressive strength $(\sigma_f)_{comp}$ (GPa)	1.25	0.54	2.06	0.78
$(\sigma_f)_{comp}/(\sigma_f)_{ten}$ (%)	37.4	12.5	58.9	27.1

showed those values in Table III. For comparison, the tensile strength and the ratio of compressive strength to the tensile strength are also shown in Table III. The estimated real compressive strength of PAN-based carbonized fiber (higher strength type) is the highest and pitch-based carbon fiber follows. For both PAN-based and pitch-based fibers, the estimated compressive strength of graphitized fiber (higher modulus type) is always less than half of that of carbonized fiber (higher strength type). Furthermore, the ratio of compressive strength to the tensile strength is approximately 35–60% for carbonized fibers, while its ratio is approximately 10–25% for graphitized fibers. It is noted that the estimated real compressive strength of graphitized fiber is remarkably low.

Hawthorne and Teghtsoonian[3] reported that the compressive strength $(\sigma_f)_c$ of pitch-based carbon fiber depends on its Young's modulus. According to their study, the compressive strength $(\sigma_f)_c$ is constant, about 2.3 GPa, in Young's modulus ranges of 130–330 GPa. Furthermore, when Young's modulus of the fiber is 450 GPa $(\sigma_f)_c$ decreases to 1.2 GPa. On the other hand, the compressive strength $(\sigma_f)_c$ of PAN-based carbon fiber with Young's modulus of 340 GPa is 2.1 GPa. These values are approximately double what we obtain. It is conceivable that these differences may be caused by their assumption that the compressive modulus is the same value as Young's modulus and the carbon fibers in compression show Hooken's behaviour.

Kitano et al.[8] obtained the compressive strength $(\sigma_f)_c$ of about 4.4 GPa for PAN-based carbonized fiber (T-300) and about 2.8 GPa for PAN-based graphitized fiber (M-40) by using the loop method.[2] Moreover, $(\sigma_f)_c$ of about 1.3 GPa was obtained for pitch-based fiber. In their report, the tensile strength of carbonized fiber (T-300) is 3.53 GPa and that of graphitized fiber (M-40) is 2.74 GPa. The obtained compressive strength is higher than the tensile strength. We consider that the compressive strength of the carbon fibers is lower than the tensile strength owing to the fiber structure. The results obtained by Kitano et al. are completely in contrast to our experimental results.

CONCLUSIONS

If a sufficiently long fiber is embedded in the neighborhood of the surface of rectangular beam and the system is subjected to a tensile (or compressive) strain greater than the fiber ultimate strain according to the bending method, the fiber eventually breaks into many pieces. Measuring the lengths of the

broken pieces, attempts were made to estimate the axial compressive strength of carbon fibers.

The estimated compressive strength of carbon fibers decreases with increasing temperature range from room temperature to 100°C. This decrease in compressive strength may be accounted for by a decrease in the radial compressing force owing to (1) decrease in residual thermal stress and (2) a decrease in Young's modulus of the resin matrix. On the other hand, the estimated compressive strength increases greatly with increasing temperature above 120°C. This increase in compressive strength may be accounted for by unsubjecting to accurately a compressive strain owing to the fiber buckling occurring with more of a decrease in Young's modulus of the resin matrix.

There is a linear relationship between the estimated compressive strength and radial compressing force in a temperature range from room temperature to 100°C. The real compressive strength of the fibers, determined by extrapolating this straight line until the radial compressing force is zero, approximately 25–60% of tensile strength for PAN-based fibers, while it is approximately 10–35% for pitch-based fibers.

References

1. J. H. Sinclair and C. C. Chamis, *Compression Testing of Homogeneous Materials and Composites*, ASTM STP 808, ASTM, Philadelphia, 1983, p. 155.

2. W. R. Jones and J. W. Johnson, *Carbon*, **9**, 645 (1971).

3. H. M. Hawthorne and E. Teghtsoonian, *J. Mater. Sci.*, **10**, 41 (1975).

4. A. Kelly and W. R. Tyson, *J. Mech. Phys. Solids*, **13**, 329 (1965).

5. A. Kelly and W. R. Tyson, *J. Mech. Phys. Solids*, **14**, 177 (1966).

6. T. Ohsawa, A. Nakayama, M. Miwa, and A. Hasegawa, *J. Appl. Polym. Sci.*, **22**, 3203 (1978).

7. G. Gerard and A. C. Gilbert, *J. Appl. Mech. (ASME)*, **24**, 355 (1957).

8. A. Kitano, T. Norita, and K. Noguchi, *12th Fukugo Zairyo Symp. Kohen-Yoshishu*, 125 (1987).

Received August 31, 1989
Accepted September 6, 1989